Characterization and properties of ZrO$_2$-forsterite composites from zircon and magnesite via reaction sintering

Lei Yuan[a], Beiyue Ma[a,]*, Yulong Du[a], Guangqiang Li[b], Qiang Zhu[c] and Jingkun Yu[a]

[a]*School of Metallurgy, Northeastern University, Shenyang 110819, P. R. China*
[b]*The State Key Laboratory of Refractories and Metallurgy, Key Laboratory for Ferrous Metallurgy and Resources Utilization of Ministry of Education, Wuhan University of Science and Technology, Wuhan 430081, P. R. China*
[c]*Electron Microscope Unit, Mark Wainwright Analytical Centre, The University of New South Wales, Sydney, NSW 2032, Australia*

ZrO$_2$-forsterite composites have been successfully prepared from zircon and magnesite powders utilizing reaction sintering process at temperatures of 1350 ^{o}C, 1450 ^{o}C and 1550 ^{o}C. The weight stoichiometric ratio of calcined magnesite and zircon to form forsterite is 31.6 : 68.4, however, in order to study the effects of calcined magnesite on the sintering behavior and properties of the composites, excessive amounts of calcined magnesite powder by 10%, 20% and 40% have also been added in the starting materials respectively. XRD results show that the phase of zirconia in the sintered composites transforms from monoclinic to cubic with increasing the amounts of calcined magnesite powder. SEM observations reveal that increasing sintering temperature is beneficial to the densification of ZrO$_2$-forsterite composites. And increasing the excessive amount of calcined magnesite can result in an improvement of thermal shock resistance ability but the decrease of the cold crushing strength in the ZrO$_2$-forsterite composites.

Key words: Zirconia, Forsterite, Reaction sintering process, Magnesite, Zircon.

Introduction

Forsterite (Mg$_2$SiO$_4$), a member of olivine family, possesses a number of outstanding properties, such as high melting point (1890 ^{o}C), low thermal conductivity, good chemical stability, low dielectric constant and excellent biocompatibility [1-4]. Such promising properties have enabled forsterite a wide range of applications, e.g., refractory materials, steel coatings, dielectric substrates, optical devices, biomaterials, *etc* [5-10]. There are various methods available to prepare forsterite materials, including reaction sintering process, microwave sintering, sol-gel method, mechanically activated process and molten salt technique [11-14]. In recent years, due to increasing demands for higher performance of forsterite materials, various types of forsterite composites, for example forsterite-mullite, forsterite-spinel, forsterite-Al$_2$O$_3$, forsterite-cordierite and forsterite-ZrO$_2$, *etc* [15-19] have been successfully developed.

Zirconia possesses a high melting point, excellent chemical inertness and corrosion resistance, high strength and good thermal conductivity [20]. When doped with some kinds of stabilizer, i.e. MgO, CaO, Y$_2$O$_3$ and CeO$_2$, zirconia materials could exhibit further excellent mechanical and electrical properties, superior

thermal shock resistance ability [21]. As forsterite contains MgO, ZrO$_2$-forsterite composite materials which have been prepared utilizing MgO to modify the crystal structure are expected to have further improved properties, such as the thermal shock resistance.

The common process to fabricate ZrO$_2$-forsterite composites is solid-state sintering method using forsterite and zirconia as raw materials. In recent years, the reaction sintering process has been considered as a promising technology because it is an easier production technology, and more importantly it can significantly reduce the manufacturing cost as it uses cheaper raw materials [22].

Magnesite is a mineral mainly containing MgCO$_3$, which can be calcined to obtain MgO. It is reported that the total reserve of magnesite in China reaches up to 3.1×10^9 tons [23]. The main application is to fabricate refractories. Zircon mainly consists of ZrO$_2$ and SiO$_2$. So far, the present reserve of zircon (calculated from ZrO$_2$) is about 3.2×10^7 tons worldwide, and zircon has been mainly used to fabricate ceramic, glass and refractories [24]. However, there are few studies at present on the preparation of ZrO$_2$-forsterite composites utilizing magnesite and zircon as raw materials [25].

Therefore, in the current study, authors have successfully prepared ZrO$_2$-fosterite composites using magnesite and zircon as raw materials by the reaction sintering process. The effects of sintering temperature and amounts of calcined magnesite on the phase composition, sintering behavior, microstructure, mechanical strength

*Corresponding author:
Tel : +86-24-83670436
Fax: +86-24-83681576
E-mail: maby@smm.neu.edu.cn

and thermal shock resistance have been investigated, and the formation process of ZrO_2-forsterite composite has been discussed as well. The present work aims to study sintering behavior and properties of ZrO_2-forsterite composite by direct reaction sintering process and provide a route with low manufacturing cost.

Experimental

Raw materials and preparation process

Magnesite (mesh size $\leq 80\ \mu m$) and zircon (mesh size $\leq 44\ \mu m$) were chosen as raw materials. The chemical compositions of the raw materials are listed in Table 1. As magnesite releases CO_2 gas in the samples which could prevent the densification of the composites during the sintering process, magnesite was firstly calcined at 750 °C for 2hrs. The overall reaction equation for synthesizing ZrO_2-forsterite composites using calcined magnesite and zircon can be described by the following equation.

$$ZrSiO_4(s) + 2MgO(s) = ZrO_2(s) + Mg_2SiO_4(s) \qquad (1)$$
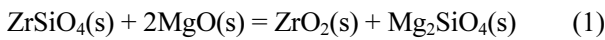
According to Eq. (1), the weight stoichiometric ratio of calcined magnesite and zircon is 31.6 : 68.4. In order to study the effects of amounts of calcined magnesite on the sintering behavior and properties of the fabricated composites, excessive calcined magnesites with 10%, 20% and 40% were also added and studied. The ratios of raw materials of the samples are listed in Table 2. Various amounts of calcined magnesite and zircon were mixed initially, then ball-milled in ethanol for 24 hrs using zirconia balls. After fully mixing and drying, the powders were pressed to form cylindrical samples with 20 mm in diameter and 20 mm in height under a 200 MPa pressure using a steel die. Then the cylindrical samples were placed in an electric furnace and sintered in air atmosphere at 1350 °C, 1450 °C and 1550 °C for 4hrs with a heating rate of 4 °C/min, respectively. The sintered samples were naturally cooled down to room temperature in the furnace and then the

Table 1. Chemical composition of the raw materials (wt%).

Raw materials	ZrO₂	SiO₂	Al₂O₃	TiO₂	Fe₂O₃	CaO	MgO	I.L.
Magnesite	–	0.65	0.18	–	0.23	1.53	47.02	50.39
Zircon	66.05	33.24	0.42	0.15	0.10	0.02	0.02	–

Table 2. Ratio of raw materials of the samples (wt%).

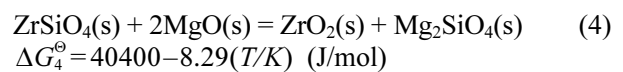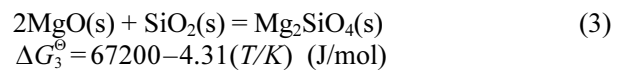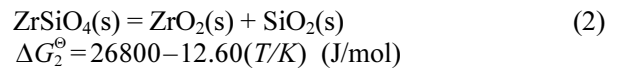| Samples	Calcined magnesite	Zircon
S1	31.6	68.4
S2	33.7	66.3
S3	35.7	64.3
S4	39.3	60.7

fabricated ZrO_2-forsterite composites were obtained.

Characterization

Apparent porosity and bulk density of all samples were determined by the Archimedes method with water as the medium. The volume shrinkage ratio of the samples was also determined and calculated. Phase compositions were identified by X-ray powder diffraction (XRD, Model D500, Siemens) using Cu K_α radiation. The microstructure and morphology of composites were observed by scanning electron microscope (SEM, Model JSM-6400, JEOL, Japan) equipped with an X-ray energy dispersive spectroscopy (EDS, Oxford, UK) unit. Cold crushing strength was measured by using hydraulic press machine (5015 type, China) according to GB/T 5072-2008 Standard. The thermal shock test was carried out by water quenching method at 1200 °C for 0.5 h to record the cycles until the samples were cracked.

Results and Discussion

Phase composition

Fig. 1 shows the XRD patterns of all the samples sintered at 1350 °C, 1450 °C and 1550 °C for 4 hrs, respectively. It can be observed that the zircon phase is not detected in all the samples, even in the samples sintered at 1350 °C. For this case, the chemical reactions (Eq. 2-4) were likely to occur during the sintering process and the relationship between $\Delta G^{\ominus}$ and T ($\Delta G^{\ominus}$-T) can be expressed as follows [24].

$$ZrSiO_4(s) = ZrO_2(s) + SiO_2(s) \qquad (2)$$
$$\Delta G_2^{\ominus} = 26800 - 12.60(T/K)\ \ (J/mol)$$

$$2MgO(s) + SiO_2(s) = Mg_2SiO_4(s) \qquad (3)$$
$$\Delta G_3^{\ominus} = 67200 - 4.31(T/K)\ \ (J/mol)$$

$$ZrSiO_4(s) + 2MgO(s) = ZrO_2(s) + Mg_2SiO_4(s) \qquad (4)$$
$$\Delta G_4^{\ominus} = 40400 - 8.29(T/K)\ \ (J/mol)$$

Since the reactants and the products were pure solids, there activity could be chosen as 1. Then, the theoretical decomposition temperature of zircon could be calculated as about 1854 °C. However, when the calcined magnesite exists in the samples, zircon can be decomposed and react with MgO completely in the whole range of sintering temperatures. That is to say it is feasible in thermodynamics to form ZrO_2-forsterite composites at the sintering temperatures.

For the case of the ratio of calcined magnesite and zircon was 31.6 : 68.4 and the sintering temperature 1350 °C, the main crystalline phases after sintering were Mg_2SiO_4, m-ZrO_2 and small amounts of t-ZrO_2, as shown in S1 in Fig. 1(a). The existence of t-ZrO_2 indicates that MgO has been dissolved in ZrO_2. With increasing the sintering temperature, as shown in S1 in
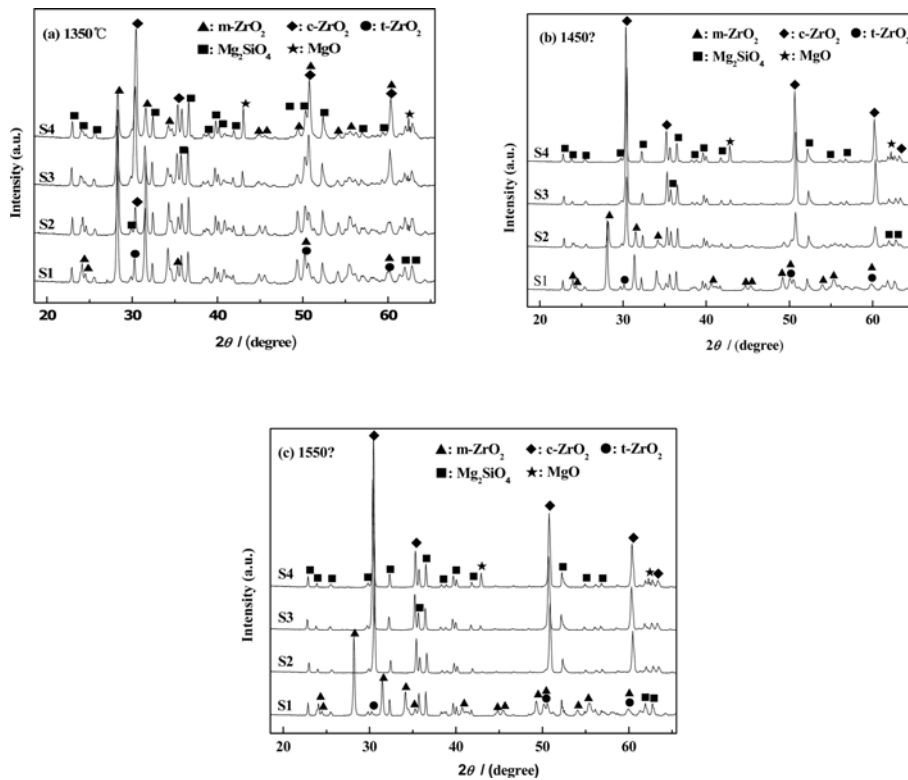
Fig. 1. The XRD patterns of the samples sintered at different temperatures for 4 hrs: (a) 1350°C, (b) 1450°C, (c) 1550°C

Fig. 1(b) and Fig. 1(c), the intensity of m-ZrO_2 phase increases and t-ZrO_2 phase decreases. It can be explained that MgO reacted with zircon thoroughly at higher sintering temperatures resulting in less amounts of MgO dissolved in ZrO_2. As for the cases of increasing the content of calcined magnesite, as shown in S2, S3, S4 of Fig. 1(a), the intensity of m-ZrO_2 decreases and c-ZrO_2 increases gradually, and small amounts of periclase phase appear. It should be noted that the m-ZrO_2 phase disappears gradually in those samples sintered at higher temperatures, which indicates that the residual MgO has been dissolved in ZrO_2 to modify the crystal structure forming c-ZrO_2 phase finally. And with increasing the sintering temperature, all of the ZrO_2 phase has been totally transformed into c-ZrO_2 resulting in the disappearance of m-ZrO_2 phase. In consequence, ZrO_2-forsterite composites can be prepared at 1350-1550°C from zircon and calcined magnesite by reaction sintering process.

Sintering behaviors

Fig. 2 compares the volume shrinkage ratio of all the samples after sintering at different temperatures for 4hrs. It can be seen that the volume shrinkage ratio of all the samples is promoted gradually with increasing the sintering temperature. For the sample S1 sintered at 1550 °C, the volume shrinkage ratio reaches 34.4%. However, when the amounts of calcined magnesite increase, as shown in S2, S3, S4 of Fig. 2, the volume
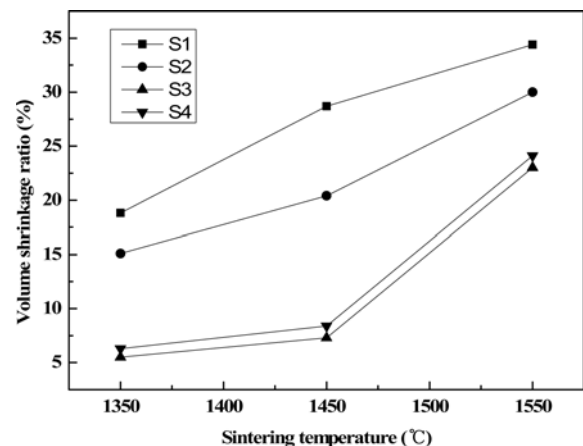

Fig. 2. The volume shrinkage ratio of the samples sintered at different temperatures for 4 hrs

shrinkage ratio decreases markedly. It seems that the excessive amounts of calcined magnesite have an effective influence on the densification of ZrO_2-forsterite composites. Fig. 3 shows the apparent porosity and bulk density of the samples sintered at different temperatures. It can be seen that the apparent porosities decrease and bulk density increases with increasing the sintering temperature. When the raw materials ratio of calcined magnesite and zircon is 31.6 : 68.4 and the sintering temperature is 1550 °C, the apparent porosity is only 3.2% and bulk density reaches 3.78 g/cm^3. Whereas, the excessive amount of calcined magnesite is considered as
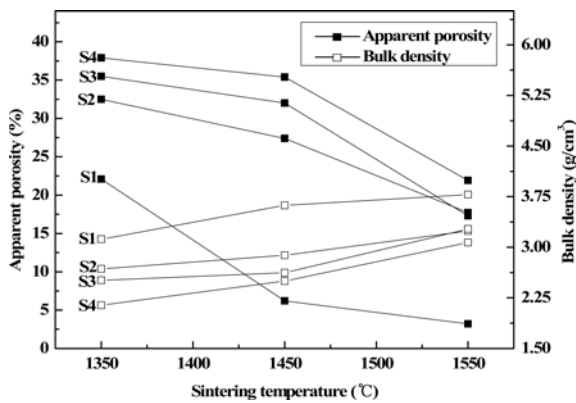
Fig. 3. The apparent porosity and bulk density of the samples sintered at different temperatures for 4 hrs

a disadvantage to the densification of the composites leading to the increasing of apparent porosity and the decreasing of bulk density. The results are consistent with the tendency of volume shrinkage ratio. In the current case, MgO reacts not only with SiO_2 to form forsterite, small amounts of MgO also can be dissolvable in the crystal lattice of ZrO_2 in the MgO-ZrO_2-SiO_2 system. When the calcined magnesite and zircon are mixed at the stoichiometric ratio of 31.6 : 68.4, small amounts of residue SiO_2 as well as the impurities of the raw materials can be existed in the system to form liquid phase sintering resulting in the densification of ZrO_2-forsterite composites. However, once the amounts of calcined magnesite are excessive, all amounts of SiO_2 will react with MgO to form forsterite and reaction solid state sintering will be dominant leading to a relatively high porosity structure.

Microstructure

Fig. 4 shows the backscattered SEM images of all the samples fabricated at different temperatures. It can be found that the zirconia grains (bright grains) are homogeneously distributed in the forsterite matrix (grey grains). For sample S1 sintered at different temperatures, as shown in Figs. 4(a-c), the zirconia crystalline grain size is about 1-5 μm which increases gradually with promoting the sintering temperature. And the density of pores decreases gradually in the matrix with increasing the sintering temperature. It indicates that the higher sintering temperature can improve the growing up of crystalline grains and the densification of the composites. This result is consistent with the apparent porosities of samples. However, after adding excessive amounts of calcined magnesite, as shown in Figs. 4(d-f), c-ZrO_2 phase appears due to the dissolve of MgO into zirconia crystalline. Moreover, it can also be seen that a relatively porous microstructure has been found in the samples with increasing excessive amounts of calcined magnesite. Therefore, promoting the sintering temperature
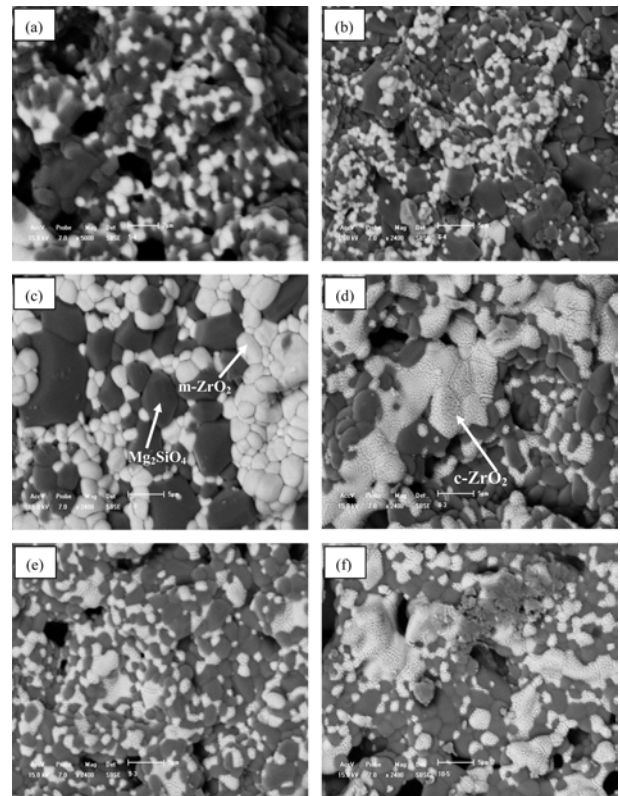
Fig. 4. Backscattered SEM images of the samples sintered at different temperatures: (a) S1 1350 ᵒC, (b) S1 1450 ᵒC, (c) S1 1550 ᵒC, (d) S2 1550 ᵒC, (e) S3 1550 ᵒC, (f) S4 1550 ᵒC.
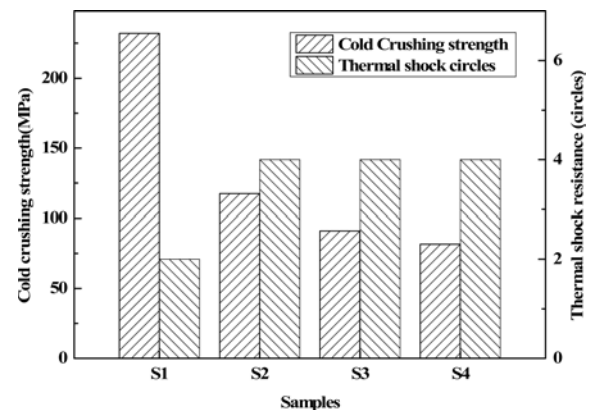
Fig. 5. The cold crushing strength and thermal shock resistance of samples sintered at 1550 ᵒC for 4 hrs.

and adding appropriate amounts of calcined magnesite are beneficial to the densification of ZrO_2-forsterite composites.

Mechanical and thermal properties

Fig. 5 shows the cold crushing strength and thermal shock resistance of the samples sintered at 1550 ᵒC for 4hrs. The cold crushing strength reaches 232.1MPa when the weight ratio of calcined magnesite and zircon is 31.6 : 68.4 (sample S1). As the amounts of calcined magnesite in raw materials increased, the cold crushing strength decreased markedly. The main reason is that a

relatively high porosity exists in the samples S2, S3 and S4 resulting in a lower strength.

Simultaneously, the water quenching circles of S1 for the thermal shock resistance testing are only two, which is less than that of the samples S2, S3 and S4. The reasons can be attributed to two aspects. On the one hand, more pores exist in the composites matrix in the samples S2, S3 and S4, which can release the thermal stress after thermal shock. On the other hand, c-ZrO_2 phase forms in the composites during the sintering and remains at room temperature when the amounts of calcined magnesite are excessive. However, the phase of ZrO_2 in sample S1 is initially monoclinic at room temperature. When the sample S1 was heated to 1200 °C, which was the thermal shock temperature, the monoclinic ZrO_2 transformed to tetragonal ZrO_2, but during cooling in water, the tetragonal ZrO_2 transformed to monoclinic ZrO_2 again accompanying 7% volume expansion. As the result, the composites are easier to crack leading to inferior thermal shock resistance.

Conclusions

(1) ZrO_2-forsterite composites have been successfully prepared at 1350-1550 °C utilizing reaction sintering process with zircon and magnesite powder as the raw materials. Zirconia grains are homogeneously distributed in forsterite matrix, and the grain size of zirconia is around 1-5 μm.

(2) Densified ZrO_2-forsterite composites can be fabricated at 1550 °C with the stoichiometric ratio of calcined magnesite and zircon. As the amounts of calcined magnesite increasing, the volume shrinkage ratio and bulk density decreased and the apparent porosity increased.

(3) Owing to the forming of c-ZrO_2 and the existing of pores in the composites matrix, the thermal shock resistance ability improved markedly in the samples with adding excessive amounts of calcined magnesite.

Acknowledgments

References

1. S. Ramesh, S.S. Tan, L.T. Bang, C.Y Tan, J. Purbolaksono, S. Ramesh, W.D. Teng, J. Ceram. Process. Res. 16[6] (2015) 722-728.
2. E. Bernardo, L. Fiocco, G.A. Giffin, V. Di Noto, P. Colombo, Adv. Eng. Mater. 16[6] (2014) 806-813.
3. K.Y.S. Lee, K.M.C. Chin, S. Ramesh, J. Purbolaksono, M.A. Hassan, M. Hamdi, W.D. Teng, J. Ceram. Process. Res. 14[1] (2013) 131-133.
4. S.Y. Ni, L. Chou, J. Chang, Ceram. Int. 33[1] (2007) 83-88.
5. T.W. Cheng, Y.C. Ding, J.P. Chiu, Miner. Eng. 15[4] (2002) 271-275.
6. S.N. Hosseini, H.S. Jazi, M. Fathi, Mater. Lett. 143 (2015) 16-19.
7. T.S. Sasikala, M.N. Suma, P. Mohanan, C. Pavithran, M.T. Sebastian, J. Alloy. Compd. 461 (2008) 555-559.
8. H.T. Sun, M. Fujii, N. Nitta, M. Mizuhata, H. Yasuda, S. Deki, S. Hayashi, J. Am. Ceram. Soc. 92 (2009) 962-966.
9. S.A. Hassanzadeh-Tabrizi, A. Bighamb, M. Rafienia, Mater. Sci. Eng. C 58 (2016) 737-741.
10. M. Kharaziha, M.H. Fathi, Ceram. Int. 35 (2009) 2449-2454.
11. A.G.M. Othman, N.M. Khalil, Ceram. Int. 31[8] (2005) 1117-1121.
12. L.G. Chen, G.T. Ye, W.H. Zhou, J. Dijkmans, B. Sels, A. Malfliet, M.X. Guo, Ceram. Int. 41 (2015) 12651-12657.
13. H.B. Bafrooei, T. Ebadzadeh, H. Majidian, Ceram. Int. 40[2] (2014) 2869-2876.
14. C.H. Han, Z.F. Wang, X.T. Wang, H.Liu, Y. Ma, M.J. Chen, Rare Metal Mat. Eng. 44[1] (2015) 515-519.
15. H. Samadi, E. Garcia, Ceram. Int. 40[9] (2014) 13995-13999.
16. E. Mustafa, N. Khalil, A. Gamal, Ceram. Int. 28[6] (2002) 663-667.
17. F.N. Cunha-Duncan, H. Balmori-Ramirez, C.C. Sorrell, R.C. Bradt, Miner. Metall. Proc. 20[3] (2003) 143-152.
18. H.K. Zhu, H.Q. Zhou, Y. Xie, M. Liu, J. Mater. Sci. - Mater. Electro. 21[3] (2010) 231-235.
19. C. Peng, N. Li, B. Han, Sci. Sinter. 41 (2009) 11-17.
20. R.H.J. Hannink, P.M. Kelly, B.C. Muddle, J. Am. Ceram. Soc. 83[3] (2000) 461-487.
21. D. Taufik, M. Abdullah, Hernawan, S. Sutardi, R. Septawendar, J. Ceram. Process. Res. 17[10] (2016) 1063-1067.
22. C.Y. Chen, G.S. Lan, W.H. Tuan, J. Eur. Ceram. Soc. 20[14-15] (2000) 2519-2525.
23. Y.N. Zhao, G.C. Zhu, Int. J. Miner. Process. 126[10] (2014) 35-40.
24. B.Y. Ma, Y. Li, S.G. Cui, Y.C. Zhai, T. Nonferr. Metal. Soc. 20[12] (2010) 2331-2335.
25. M.M.S. Wahsh, A.G.M. Othman, S. Abd El-Aleem, J. Ind. Eng. Chem. 20 (2014) 3984-3988.